Chemistry & Biology
Article

Synthetic Mimetics of Actin-Binding Macrolides: Rational Design of Actin-Targeted Drugs

Richard D. Perrins,[1] Giuseppe Cecere,[2] Ian Paterson,[2] and Gerard Marriott[1,*]
[1]Department of Physiology, University of Wisconsin, 1300 University Avenue, Madison, WI 53706, USA
[2]Department of Chemistry, Cambridge University, Lensfield Rd, Cambridge, CB2 1EW, United Kingdom
*Correspondence: marriott@physiology.wisc.edu
DOI 10.1016/j.chembiol.2008.01.010

SUMMARY

Actin polymerization and dynamics are involved in a wide range of cellular processes such as cell division and migration of tumor cells. At sites of cell lysis, such as those occurring during a stroke or inflammatory lung diseases, actin is released into the serum where it polymerizes, leading to problems with clot dissolution and sputum viscosity. Therefore, drugs that target these actin-mediated processes may provide one mechanism to treat these conditions. Marine-organism-derived macrolides, such as reidispongiolide A, can bind to, sever, and inhibit polymerization of actin. Our studies show that the function of these complex macrolides resides in their tail region, whereas the head group stabilizes the actin-drug complex. Synthetic compounds derived from this tail region could therefore be used as a mimetic of the natural product, providing a range of designer compounds to treat actin-associated diseases or as probes to study actin polymerization.

INTRODUCTION

Spatiotemporal regulation of actin filament dynamics is required for essential cell processes, including motility, endocytosis, cytokinesis, and establishing cell-cell and cell-substrate contacts (Westphal et al., 1997). Therefore, drugs that block the regulation of actin filament dynamics within tumor cells or cells infected with *Listeria* and related pathogens could prove useful in treating cancer and diseased states (Fenteany and Zhu 2003). Furthermore, cell lysis associated with stroke, malaria (Smith et al., 1988), and necrosis increases plasma actin, which can polymerize close to the site of the wound impeding clot dissolution (Haddad et al., 1990). The capacity of plasma gelsolin to neutralize actin filaments in the serum is very limited and often overwhelmed following a serious stroke (Mounzer et al., 1999). Therefore, a small molecule mimetic of plasma gelsolin would serve as a powerful drug to control plasma actin.

Marine-organism-derived macrolides, including ulapualide A (Roesener and Scheuer, 1986), kabiramide C (Petchprayoon et al., 2006; Tanaka et al., 2003), and reidispongiolide A (**1**) (Figure 1) (D'Auria et al., 1994), hereafter referred to as reidispongiolide, exert their potent cytotoxicity by causing dysfunctional regulation of actin filament dynamics in cells (Tanaka et al., 2003; Yeung and Paterson, 2002). The structural basis for the severing and (+)-end-capping activities of actin-targeting macrolides was established through biochemical and high-resolution structural studies (Allingham et al., 2005; Klenchin et al., 2003; Petchprayoon et al., 2006; Tanaka et al., 2003). Reidispongiolide and related macrolides form stable complexes with actin, having dissociation constants in the nanomolar range. In vitro and in vivo studies showed that macrolide-actin complexes reduce free G-actin to below the critical concentration, block extension of the (+)-end of the filament, while the free macrolide can also bind to and sever actin filaments (Tanaka et al., 2003). In living cells, the combined effects of these interactions leads to a cessation of new filament growth and a disruption of existing filaments and is accompanied by a loss of motility, breakdown of adherens junctions, polyploidy, and ultimately apoptosis (Tanaka et al., 2003).

Both the capping and severing activities of reidispongiolide (Figure 1) are mediated through hydrophobic interactions of the macrolide ring at the entrance of the cleft that forms at the interface of actin subdomains-1 (SD1) and -3 (SD3) and the tail region with residues that line the cleft (Allingham et al., 2005; Klenchin et al., 2003). Elongation of actin filaments requires an interaction of the DNase I binding loop (SD2) of the incoming actin monomer with residues in the hydrophobic cleft of the protomer at the (+)-end of the filament. However, the binding of the macrolide tail to the (+)-end actin protomer prevents this interaction (Allingham et al., 2005) and thereby blocks polymerization. The free macrolide can also disrupt the interaction between the D-loop and the cleft of actin monomers within the filament, leading to severing and subsequent capping of the newly formed (+)-end by the macrolide (Allingham et al., 2005; Tanaka et al., 2003).

As marine macrolides are isolated from protected organisms and typically have extremely low natural abundance, we decided to explore their interactions and activities with actin by using fully synthetic analogs of the tail region of reidispongiolide, with a view to evaluating their potential as drugs for the treatment of actin-associated disorders. Furthermore, since the tail segments of reidispongiolides A and B, sphinxolides A, B, C, and D, halichondramide, kabiramide C, mycalolide A, and jaspisamide A are structurally similar (Allingham et al., 2005; Tanaka et al., 2003), these synthetic analogs would serve as a model to study structure-function relationships within actin and as molecular probes for in vitro and in vivo studies of actin filament dynamics. A related study has been reported on simplified analogs of the aplyronine family of marine macrolides (Hirata et al., 2006; Kigoshi et al., 2002).

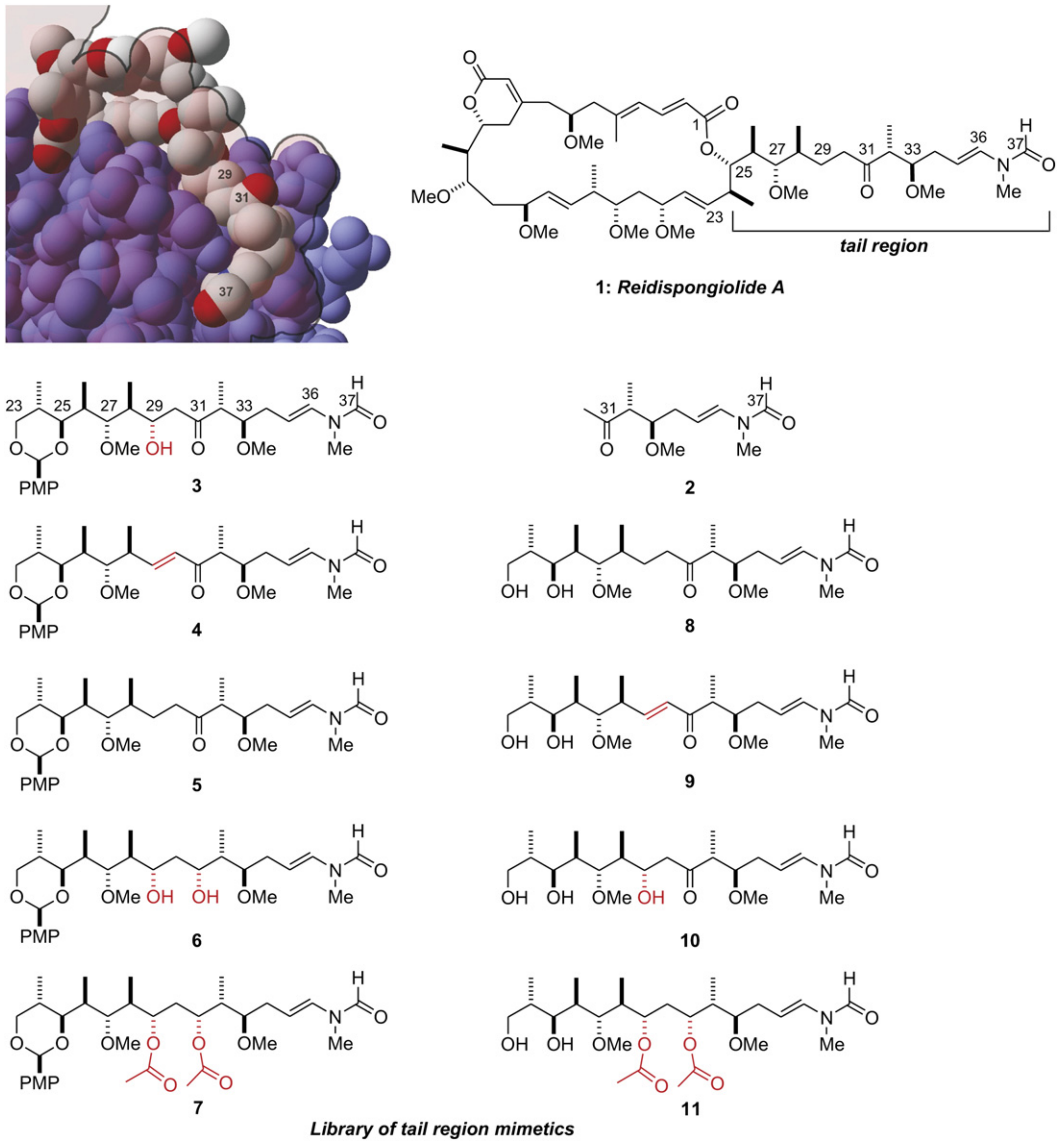

Figure 1. The Structures of Reidispongiolide A and the Tail Analogs

The chemical structures of reidispongiolide A (**1**) and the synthetic analogs based on the tail region of reidispongiolide (labeled as **2** through to **11**). Modifications to the tail are highlighted in red. Carbon atom numbering is based on the scheme previously used for reidispongiolide (Allingham et al., 2005). The crystal structure of reidispongiolide A bound to G-actin (Allingham et al., 2005) is shown in the top left. SD1 is shown in blue, SD3 is shown in translucent red, and reidispongiolide is shown in CPK coloring.

RESULTS AND DISCUSSION

The binding of G-actin with a library of chemically synthesized analogs of reidispongiolide was studied by using a highly sensitive fluorescence-based assay, detailed in Marriott et al. (1988). Use of these structurally diverse analogs allows for the definition of the interactions of specific groups on the tail with the SD1/SD3 cleft of actin and to establish the molecular determinants that underlie the binding to actin and in vitro and in vivo inhibition of actin filament dynamics. Such a small molecule would be a good starting point for the development of drugs and probes directed against actin.

Synthetic Analogs of the Tail Region of Reidispongiolide A

The library of analogs (**2**–**11**) of the tail region of reidispongiolide (**1**) employed in this study are shown in Figure 1. All of these analogs feature the characteristic *N*-vinyl formamide functionality of reidispongiolide, with conserved stereochemistry, and variation in the oxidation state at C29 and C31. The simplest analog **2** corresponds to the C30–C37 region of reidispongiolide. The more elaborate C23–C37 analogs **3**, **4**, **5**, **6**, and **7** retain a cyclic *para*-methoxybenzylidene (PMP) acetal protecting group at C23 and C25 carried over from the synthetic route, while the analogs **8**, **9**, **10**, and **11** have the liberated 1,3-diol. The synthesis of these compounds, along with

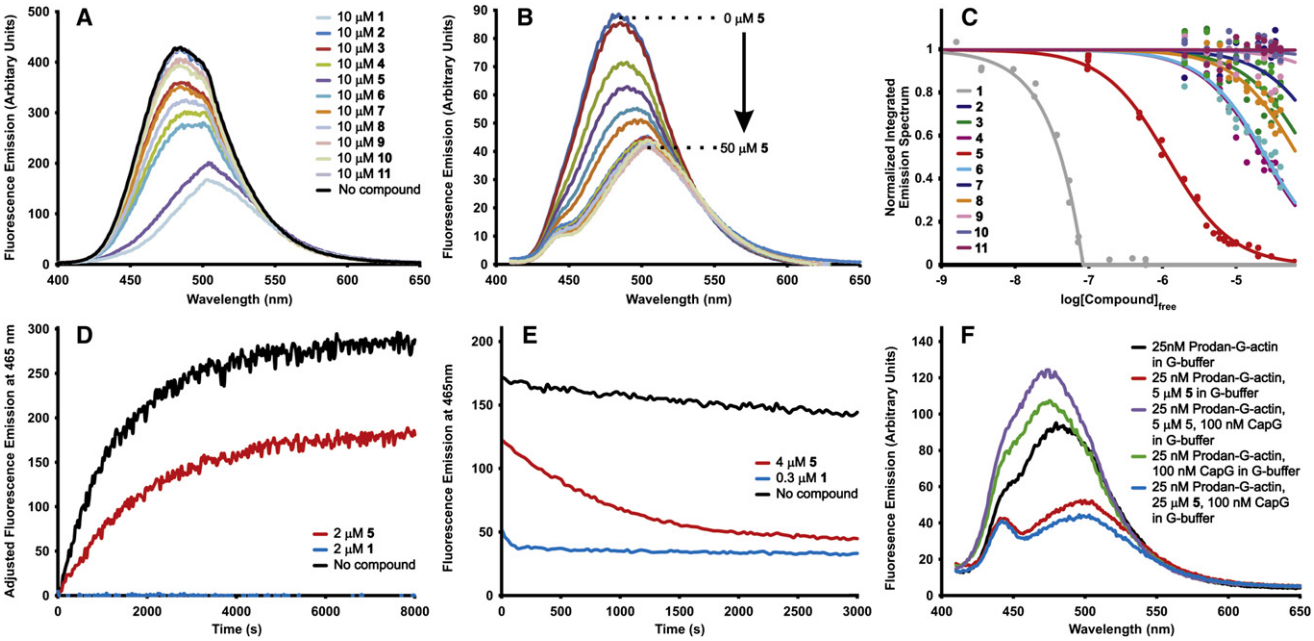

Figure 2. The Binding of Reidispongiolide and Related Compounds to Actin, Their Effect on Actin Polymerization, Depolymerization, Severing, and Competition with Other Actin-Binding Proteins

(A) Fluorescence emission spectra of 1 μM Prodan-G-actin in G-buffer and 1 μM Prodan-G-actin in G-buffer and 10 μM of compounds **1** though **11**.

(B) Incubation of 0 to 50 μM **5** with 50 nM Prodan-G-actin in G-buffer.

(C) Binding of compounds **1** through **11** to Prodan-G-actin in G-buffer. The integrated emission spectra are normalized by using the integrated spectra of Prodan-G-actin obtained in the absence of compound and in conditions where the macrolide binding site of Prodan-G-actin is fully occupied by either the compound being titrated or halichondramide. The disassociation constants are shown in Table 1.

(D) Polymerization of 2 μM Prodan-G-actin in the absence or presence of 2 μM of either **5** or reidispongiolide (**1**) in polymerization buffer.

(E) Prodan-F-actin was diluted so that the total G-actin concentration was 0.1 μM, which is below the critical concentration where actin polymerization can occur. Therefore only loss of monomers from the (−)-end is possible. The rate of depolymerization in the presence of either 4 μM **5** or 0.3 μM reidispongiolide (**1**) is significantly quicker than with just F-actin on its own. This is strongly suggestive of F-actin severing by **5** and reidispongiolide.

(F) Displacement of CapG from Prodan-G-actin by **5**.

that of reidispongiolide itself, is described elsewhere (Paterson et al., 2007, 2008).

The Tail Region Is Sufficient for Binding to G-Actin

Stoichiometric binding of reidispongiolide to Prodan-G-actin caused a characteristic red shift in the emission spectrum of Prodan and a concomitant decrease in quantum efficiency (Tanaka et al., 2003) compared to Prodan-G-actin alone (Figure 2A). A similar change is observed upon stoichiometric binding of **5** to Prodan-G-actin (Figure 2B). Since the structure of **5** is almost identical to the C25–C37 tail region of reidispongiolide, it is likely that tail binding is primarily responsible for the change in fluorescence. The same binding conditions were used to test the interaction of the other tail analogs shown in Figure 1, all of which elicited far smaller spectral shifts (Figure 2A), suggesting that these probes bound weakly to G-actin or else they did not affect Prodan fluorescence.

The Macrolide Ring Greatly Increases the Affinity of the Tail Region for Actin

To further detail the energetic contributions of the tail region to actin binding, we conducted equilibrium-binding studies for all the tail analogs, as well as for reidispongiolide itself. The intact macrolide bound stoichiometrically to G-actin even when using a Prodan-G-actin concentration of 5 nM, suggesting the K_d for this complex, as anticipated from our earlier study (Tanaka et al., 2003), is very low, i.e., less than 5 nM (Figure 2C, Table 1).

The highest affinity found among the tail analogs for G-actin was for **5** with a value of 1 μM (Figure 2C, Table 1). Since reidispongiolide binds to G-actin with an affinity that is at least two orders of magnitude higher than **5**, this stronger interaction

Table 1. Disassociation Constants of Reidispongiolide A and the Reidispongiolide Tail Analogs for Prodan-G-Actin

Compound	Disassociation Constant, K_d (μM)
Reidispongiolide A (**1**)	<0.005
2	>1,000
3	100
4	24
5	1
6	26
7	200
8	71
9	>1,000
10	>1,000
11	>1,000

must arise from the effects of cumulative binding of the ring and the tail with sites on actin. The initial binding event, which occurs with a rate of 30 s^{-1} for the intact macrolide, is associated with the change in Prodan emission (Tanaka et al., 2003). The fluorescence spectra recorded using the tail analogs in this study show that the emission is perturbed by an interaction of the tail region with G-actin and not by the macrolide ring, as we had postulated by using intact macrolides (Klenchin et al., 2003; Tanaka et al., 2003). This result was unexpected since high-resolution structures of kabirimide C-G-actin and related macrolide-actin complexes (Allingham et al., 2005; Klenchin et al., 2003) show that the tail region adopts a highly contorted conformation in the cleft where it engages stereochemically defined interactions with residues. This finding that the tail region of the macrolide binds rapidly to G-actin would suggest that the cleft is, in fact, rather open and can easily accommodate the tail analog **5**. These spectroscopic studies support our earlier conclusions (Klenchin et al., 2003; Tanaka et al., 2003) that the binding of macrolides, including reidispongiolide, to G-actin proceeds via two independent and sequential interactions that begin either with occupancy of the SD1/SD3 cleft with the tail region with an effective K_d of 71 μM followed by an interaction of the macrolide ring with the entrance of the cleft or vice versa. The effective K_d for the interaction of reidispongiolide for G-actin should therefore be described as the product of the two K_d's. Although we do not have a measure of the binding of the macrolide ring alone, the data shown in Figure 2C for reidispongiolide (**1**) and **8**, which represents the unprotected tail region, would indicate the macrolide ring binds to G-actin with a K_d in the micromolar range. This two-step binding mechanism accounts for the stability of the macrolide-G-actin complex (Tanaka et al., 2003).

Subtle Chemical Modifications within the Tail Region Affect G-Actin Binding

The truncated C30–C37 analog **2** does not exhibit any detectable binding to G-actin using our experimental system, which is sensitive to an upper K_d limit of 1.7 mM (corresponding to a 2% change or shift in the Prodan signal over a 0–40 μM concentration range and using a halichondramide-determined end point). Thus, compound **2** establishes a minimal length, being somewhere between C24 and C30 to the end of the tail, for the design of reidispongiolide-inspired tail molecules and suggests that some of the major determinants responsible for a strong interaction of the tail with actin involve regions closer to the junction with the macrolide ring.

Subtle chemical modifications within the tail region of reidispongiolide greatly influenced binding to G-actin. For example, while compound **4** differs from **5** only by a double bond at C29 to C30 (Figure 1), this change resulted in a 20-fold loss of affinity for G-actin. The rigid double bond most likely places a restriction on the flexibility of the tail around the C29–C30 linkage that would appear necessary for it to assume a twisted conformation within the SD1/SD3 cleft (Figure 1) (Allingham et al., 2005; Klenchin et al., 2003).

A more dramatic perturbation to tail binding occurs when a hydroxyl group is placed at C29 as in **3**, which results in a decrease in the dissociation constant by ~100-fold compared to **5** (Figure 2C, Table 1). Interestingly, the reduction of the ketone at C31 in **3** to the secondary alcohol in compound **6** improves the dissociation constant from 100 μM to 26 μM, respectively. An inspection of high-resolution structures of macrolides bound to G-actin (Allingham et al., 2005; Klenchin et al., 2003) shows that the ketone at C31 and the proton on C29 are both directed away from the cleft toward the solvent and do not engage in direct interactions with groups on G-actin. Therefore, we speculate that the dramatic attenuation in the K_d for the G-actin complex observed for **3** compared to **5** is a consequence of a new and stronger dipolar interaction of the hydroxyl at C29 with a residue on the cleft that directs the remaining stretch of the tail away from its normal binding site. Alternatively, the C29-hydroxyl and the ketone of **3** could form an intramolecular hydrogen bond that impairs conformational mobility and reduces the affinity of the tail for actin. The improved binding of **6** versus **3** (26 μM versus 100 μM, respectively) may reflect a greater conformational freedom around the C30-C31-C32 bonds in **6** and recovery of interactions between the tail and the cleft. Acetylation of the two secondary alcohol groups of **6** was used to generate **7**; the increased volume and hydrophobicity of the acetyl groups evidently affected specific interactions between the tail and the cleft since the K_d for the G-actin complex of compound **7** compared to **6** increased by almost an order of magnitude to 200 μM.

On the basis of the binding studies using the complete set of tail analogs, it is likely that specific hydrophobic and dipolar interactions close to the macrolide ring-tail junction are required for strong binding to G-actin and that the presence of additional polar groups or a restriction of tail flexibility greatly impedes complex formation. These results also suggest that substituent groups along the tail are inimitable, a view that is supported by the conserved structure and stereochemistry of the tail region of known macrolides (Allingham et al., 2005; Klenchin et al., 2003; Tanaka et al., 2003).

Small Apolar Groups Appended to the Tail Mimic the Macrolide Ring

The PMP acetal protecting group was removed from compounds **3**, **4**, **5**, and **7** to form the corresponding 1,3-diols **10**, **9**, **8**, and **11,** respectively (Figure 1). Removal of the aromatic PMP group greatly decreased the affinity of these compounds for G-actin, by some 71-fold in the case of **5** (Figure 2C, Table 1). The poor binding of tail analogs lacking the PMP group suggests that this acetal protecting group provides additional interactions with actin that stabilize the complex. An inspection of the high-resolution structures of actin-macrolide complexes would position the PMP group at the entrance of the SD1/SD3 cleft. We suggest therefore that the PMP group mimics in small part the contributions of the macrolide ring to the actin complex. These results and earlier studies (Allingham et al., 2005; Tanaka et al., 2003) support the idea that the complex between actin and macrolide natural products involves two independent interactions involving the tail and ring regions. The effective dissociation constant of the complex would therefore be described by the product of the K_d's for the tail and macrolide ring. Thus, in the case of the G-actin-reidispongiolide complex, the K_d for the macrolide ring alone would be at least 70 μM, the quotient of the K_d's for reidispongiolide and **8** (5 nM/71 μM). Clearly, having different polar and hydrophobic groups attached to this region could be used to modulate the affinity of the tail region for actin. Furthermore, by replacing the PMP group with

tetramethylrhodamine (a fluorophore known to have a slight affinity for the SD1/SD3 hydrophobic patch on actin; Otterbein et al., 2001) or a targeting ligand, it should be possible to generate a family of high affinity optical sensors to image the distribution of (+)-ends in live cells (Choidas et al., 1998; Petchprayoon et al., 2005) or else to target the drug to specific tumor cells.

Tail Analogs Reduce the Rate of Actin Polymerization

Salt-induced polymerization of Prodan-G-actin is accompanied by a blue shift in the Prodan emission spectra and an increase in the quantum yield that can be exploited to measure rates of actin polymerization (Marriott et al., 1988; Tanaka et al., 2003). As expected, addition of a stoichiometric level of reidispongiolide inhibited actin polymerization (Figure 2D). Similar results were found for several tail analogs although with a reduced efficacy that scaled with their effective K_d for G-actin.

Compounds exhibiting a high affinity for G-actin, such as reidispongiolide and **5**, can sequester G-actin molecules to reduce the free G-actin concentration leading to a concomitant decrease in the rate and extent of actin polymerization. For example, no actin polymerization was observed for 2 μM Prodan-G-actin in the presence of 2 μM reidispongiolide (Figure 2D), which essentially reduced the concentration of free G-actin to <5 nM or more than 40 times lower than the critical concentration for polymerization (Marriott et al., 1988). The rate for the polymerization of 2 μM Prodan-G-actin in the presence of 2 μM of **5** on the other hand was ~47% that of the control sample (Figure 2D), which given a K_d of 1 μM, would reduce the free concentration of G-actin to ~1 μM. Clearly, sequestration by **5** is not the sole mechanism for the inhibition of actin polymerization, since at this concentration compound **5** would also cap filament growth by binding to the protomer at the (+)-end of the filament and sever nascent filaments (next section).

Only the Tail Region of Reidispongiolide Is Required for Filament Severing

The rate of actin depolymerization via loss of protomers from the (+) and (−)-ends of a filament can be studied by rapidly diluting a concentrated solution of F-actin to 0.1 μM, i.e., below the critical concentration for actin polymerization (Marriott et al., 1988). Under these conditions, tail compounds added to the diluted F-actin that increase the rate of depolymerization compared to the control sample must do so by severing filaments. This property is clearly demonstrated for 2 μM of compound **5** or reidispongiolide in Figure 2E, which shows a plot of the amount of Prodan-F-actin versus time in the absence or presence of the drug. Similar results were obtained when using F-actin at 2 μM, ten times the critical concentration for actin polymerization (data not shown). No evidence of filament severing was found by using other tail derivatives up to 4 μM, although we anticipate they would exhibit a severing activity when used closer to their own K_d concentration. Studies using analogs of the macrolide aplyronine A also suggest that the actin-deplymerizing activity was mediated by the aliphatic tail (Hirata et al., 2006; Kigoshi et al., 2002).

Tail Regions of Reidispongiolide Bind to the (+)-End of the Actin Filament

CapG is a Ca^{2+}-activated actin-binding protein that forms complexes with the (+)-end of F-actin with reported K_d values between 25–100 nM (Southwick and DiNubile, 1986; Tanaka et al., 2003; Zhang et al., 2006). The fluorescence emission spectrum of Prodan-G-actin in the CapG complex is remarkably similar to that observed for F-actin, suggesting a similar buried environment for Prodan (Tanaka et al., 2003). This characteristic fluorescence spectrum was used to show that reidispongiolide and the tail analogs compete for the same site on G-actin as CapG. Thus, by using stoichiometric binding conditions, we found that **5** (20 μM) effectively displaced 100 nM CapG from its complex with 25 nM Prodan-G-actin as evidenced by a red-shifted Prodan spectrum that is similar to that found in the complex of **5** with Prodan-G-actin (Figure 2F). Stoichiometric levels of CapG were also found to displace **5** from its complex with Prodan-G-actin (Figure 2F). These results are consistent with our earlier study with kabiramide C and with later crystallographic analyses of G-actin complexes with macrolides (Klenchin et al., 2003) and (+)-end binding proteins (Dominguez, 2004) that show the tail region of the macrolide and a long α helix within the capping protein bind along the cleft that forms between SD1 and SD3 (Allingham et al., 2005).

Cell Studies

Treatment of rat bladder epithelial cells (NBT-II) with reidispongiolide at concentrations >100 nM produces similar effects as those generated by kabiramide C (Tanaka et al., 2003) with rapid disruption of actin-rich adherens junctions, breakdown of cell-cell contacts, polyploidy, and eventually apoptosis (Figure 3). The strong and long-lived G-actin complex, together with its severing and (+)-end capping activity, allows reidispongiolide to accumulate in the cell to significant levels even with a bathing concentration of 10 nM. This occurs in spite of high concentrations (>50 μM) of endogenous G-actin binding proteins, such as profilin and thymosin β4, which bind to G-actin about 100-fold less tightly compared to reidispongiolide (Goldschmidt-Clermont et al., 1990, 1992). None of the reidispongiolide tail analogs affected cell morphology or viability when used below 1 μM, nor did the weakly binding compounds **2**, **3**, **8**, **9**, **10**, and **11** at a bathing concentration of 10 μM. On the other hand, prolonged exposure (16 hr) of NBT-II cells to compounds **4** and **6** at 10 μM caused breakdown of adherens junctions, as evidenced by the loss of cell-cell contacts (Figures 3J and 3K). Compound **5**, as expected based on the equilibrium binding studies, induced dramatic morphologic changes and cytotoxicity to NBT-II cells when added to the medium at 10 μM (Figure 3I), and even at 1 μM (Figure 3H), there was evidence of a breakdown in adherens junctions. We argue that the cytotoxicity of the tail analogs scales with the dissociation constant of their complex with G-actin. Therefore, if all the tail compounds are membrane permeable, then only a tiny fraction of cell actin would exist in a complex for the very weakly binding tail analogs (**2**, **3**, **8**, **9**, **10**, **11**).

Finally, it was surprising to find that compound **7** was also effective in breaking cell-cell contacts in NBT-II epithelia, since its complex with G-actin has a poor K_d of 200 μM. The observed cytotoxicity most likely arises by hydrolysis of the two ester groups in **7** by nonspecific cellular esterases that would generate **6**, improving the affinity for G-actin by almost 8-fold. It is also significant that ulapualide A and aplyronine A also harbor large ester-linked hydrophobic groups in their tail region that should reduce their affinity for actin. In fact, ulapualide A is known to exhibit weak binding to actin that compromised assignment of the atoms

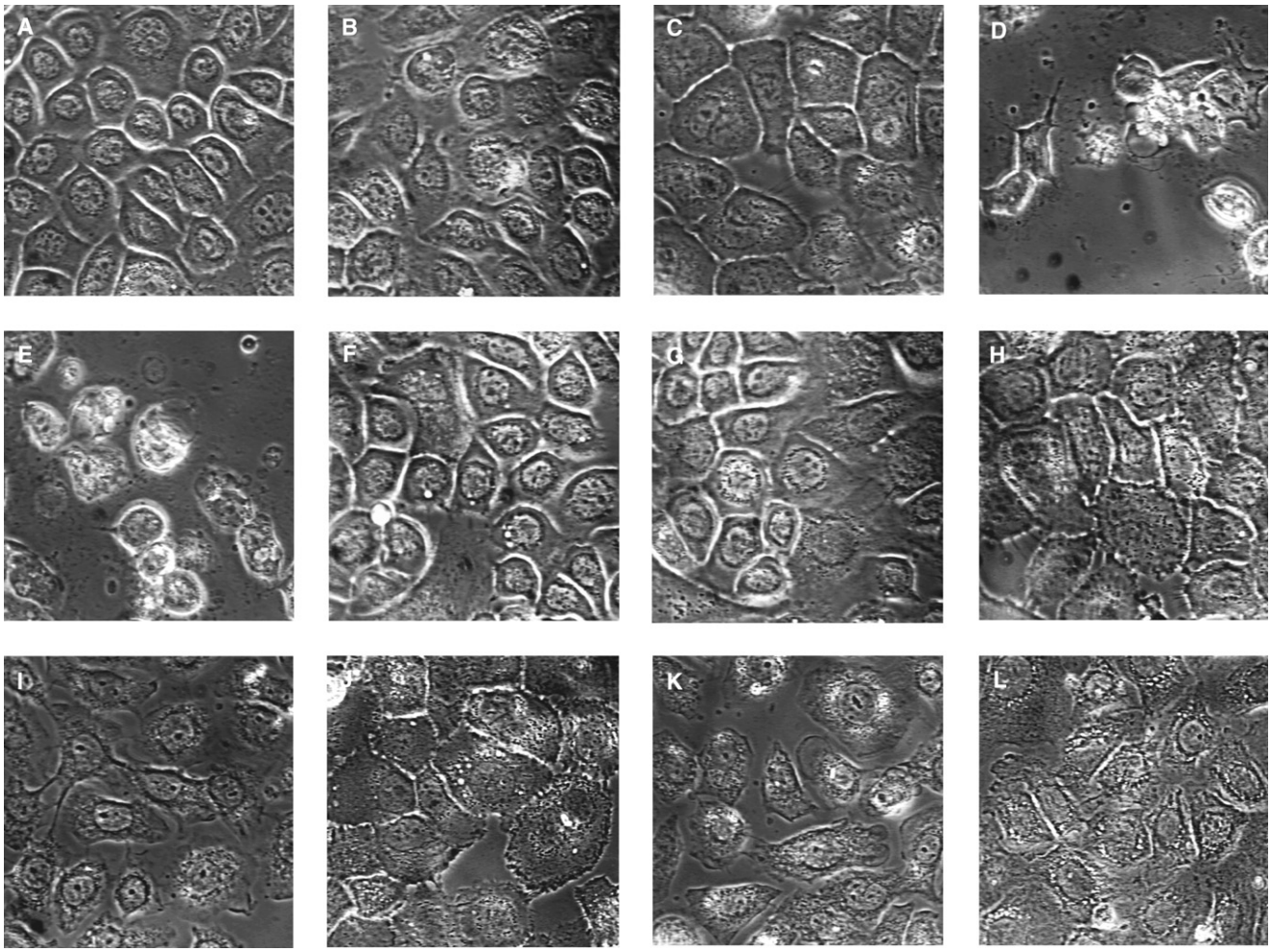

Figure 3. The Effect of Reidispongiolide and Tail Analogs 4, 5, 6, and 7 on Cultured NBT-II Cells
Micrographs of (A) untreated NBT-II epithelial cells and NBT-II cells treated with: (B) 10 nM, (C) 100 nM, (D) 1 μM, and (E) 10 μM reidispongiolide; (F) 10 nM, (G) 100 nM, (H) 1 μM, and (I) 10 μM tail analog **5**; (J) 10 μM tail analog **4**; (K) 10 μM tail analog **6**; and (L) 10 μM tail analog **7**.

in the terminal region of the macrolide tail in the high-resolution structure of the complex (Allingham et al., 2004). If the de-esterified tails of ulapualide and other macrolides were found to be the active forms of the drug in cells, then it would be prudent to conduct future structural and binding studies with these modified drugs.

SIGNIFICANCE

This study has shown that the G-actin-binding and actin-filament-severing activity observed for marine organism-derived macrolides such as kabiramide C (Tanaka et al., 2003) and reidispongiolide (Allingham et al., 2005; D'Auria et al., 1994) reside in the tail region of the molecule. We defined a minimum length of the tail (in 2) for actin binding of ~1 nm and showed that the affinity of the full-length tail analogs was attenuated by reducing conformational flexibility within the tail or by introducing a polar hydroxyl group at C29 (as in 3). The affinity of the tail region for actin, as well as the severing activity, improved dramatically on attaching a small hydrophobic protecting group (PMP) to the C23 and C25 hydroxyls. We argued that the aromatic acetal protecting group mimics the action of the macrolide ring by providing additional binding energy to the complex through a separate and sequential interaction (Allingham et al., 2005; Tanaka et al., 2003). This finding suggests that the affinity of the tail for actin could be further improved by appending larger hydrophobic groups. Attractive candidates would be tetramethylrhodamine, which would also serve as a sensitive optical probe of the barbed end in cells (Choidas et al., 1998; Petchprayoon et al., 2005), and specific ligands for receptor proteins that could be used to deliver the cytotoxic tail to specific tumor cells or to restrict the tail to serum for control of serum actin following stroke or to reduce the viscosity of sputum, produced by inflammatory lung diseases.

EXPERIMENTAL PROCEDURES

Reidispongiolide and Tail Analogs

Reidispongiolide (**1**) and its tail analogs **2**–**11** were prepared by the synthetic routes reported by Paterson et al. (2007, 2008). The compounds were dissolved in DMSO to a concentration of 2 mM and stored at −20°C.

Prodan-Actin

By using protocols that have been previously described by Marriott et al. (1988), G-actin was purified from chicken skeletal muscle and subsequently labeled with the thiol-reactive probe Acrylodan (Invitrogen). The labeling of actin with Prodan has been reported not to affect the functional activity of actin (Marriott et al., 1988; Roy et al., 2001; Zechel, 1993). Protein concentrations were measured by the Bradford assay (Bradford, 1976) and labeling efficiencies measured with an UV-1601PC UV-Visible Spectrophotometer (Shimadzu), the extinction coefficient of actin at 290 nm ($2.6 \times 10^4\ M^{-1}\ cm^{-1}$) (Gordon et al., 1976) and the extinction coefficient of Prodan at 375 nm ($1.85 \times 10^4\ M^{-1}\ cm^{-1}$) (Weber and Farris, 1979) and at 290 nm ($1.85 \times 10^4\ M^{-1}\ cm^{-1}$) (Marriott et al., 1988). Labeling efficiencies were typically around 30%.

Binding of Reidispongiolide and Its Analogs to Prodan-G-Actin

Red shifts in the fluorescence emission spectrum of Prodan-G-actin, which occur upon binding macrolides, were measured with an Aminco-Bowman Series 2 (AB2) Fluorimeter (ThermoSpectronic). For the preliminary binding experiments, the emission spectra of 1 μM Prodan-G-actin in G-buffer (2 mM Tris [pH 8], 0.2 mM ATP, 0.2 mM $CaCl_2$, 0.2 mM DTT) in the presence of 10 μM reidispongiolide, 10 μM of a compound derived from the tail region of reidispongiolide (compounds **2** through **11**) or in the absence of any additional compound were measured. These samples were excited at 385 nm (4 nm bandpass, 0° polarization), and the emission spectra measured from 400 nm to 650 nm (4 nm bandpass, 54.7° polarization).

To measure the disassociation constants, the emission spectra of G-actin, in G-buffer, in the presence of a range of compound concentrations were measured. For compounds **2** to **11**, 50 nM Prodan-G-actin was used, and 5 nM Prodan-G-actin was used when measuring the affinity for reidispongiolide. Compound concentrations ranged from 0–400 nM for reidispongiolide A and 0–40 μM for the macrolide-tail-derived compounds. Concentrations of compounds greater than 40 μM were prohibited due to the accompanying high DMSO concentration, which would lead to denaturation of Prodan-G-actin. For those compounds where 100% binding to Prodan-G-actin was not possible, the end-point spectrum was generated by measuring 50 nM G-actin in G-buffer with a saturating concentration of the macrolide halichondramide (Tanaka et al., 2003). These samples were excited at 385 nm (8 nm bandpass, 0° polarization), and the emission spectra measured from 410 nm to 650 nm (16 nm bandpass, 54.7° polarization).

For the binding of compounds **2** through to **11**, the raw emission spectra were integrated with the AB2 software (ThermoSpectronic). Due to the low intensity of the emission spectra produced with 5 nM Prodan-G-actin, the water Raman peak at ~440 nm had to be subtracted from the reidispongiolide spectra before integrating. Integrated spectra were normalized between the values obtained in the absence and presence of a saturating concentration of macrolide or tail analog. Disassociation constants were calculated by curve fitting to the normalized integrated spectra.

Polymerization of Actin in the Presence of Reidispongiolide and Its Derivatives

The time course of the polymerization of 2 μM G-actin in G-buffer, with either 2 μM reidispongiolide, tail analog, or no additional compound present, was followed with an AB2 fluorimeter. Two millimolars $MgCl_2$ and 100 mM KCl were added to the reaction to initiate polymerization immediately before the samples were inserted into the fluorimeter. Samples were excited at 385 nm (4 nm bandwidth, 0° polarization), and the emission was measured at 465 nm (4 nm bandwidth, 54.7° polarization).

Severing Assay in the Presence of Actin Polymerization

2.2 μM G-actin was allowed to polymerize overnight in polymerization buffer (2 mM Tris [pH 8], 0.2 mM ATP, 0.2 mM $CaCl_2$, 0.2 mM DTT, 2 mM $MgCl_2$, 100 mM KCl) at 4°C. The polymerized actin was diluted, to produce a total monomer concentration of 2 μM, in polymerization buffer that contained 2–4 μM reidispongiolide, 2–4 μM tail analog, or no additional compound. Severing and depolymerization of the F-actin was followed with an AB2 fluorimeter with the settings used to measure actin polymerization (see above).

Severing/Depolymerization Assay in the Absence of Further Actin Polymerization

Two micromolars G-actin was allowed to polymerize overnight in polymerization buffer at 4°C. The polymerized actin was diluted, to produce a total monomer concentration of 0.1 μM, in polymerization buffer that contained 4 μM reidispongiolide, 4 μM of **5** or no additional compound. Severing and depolymerization of the F-actin was followed with an AB2 fluorimeter under the same settings as used to measure actin polymerization (see above).

CapG Competition Binding Assay

CapG was purified, from bacteria expressing CapG cDNA, as previously outlined in Tanaka et al. (2003). CapG protein was stored as a glycerol stock at −20°C. Before use, glycerol stocks of CapG were dialyzed overnight against G-buffer, at 4°C, and protein concentrations measured by the Bradford assay (Bradford, 1976).

To measure the competition of the two compounds for actin, fluorescence emission spectra were taken of: (1) G-actin in G-buffer; (2) G-actin and the compound to be displaced in G-buffer; (3) G-actin and the displacing compound in G-buffer; (4) G-actin, the displaced compound, and the displacing compound in G-buffer. The compound to be displaced was present at approximately its K_d for G-actin, the displacing compound was present at 20 times its K_d for G-actin, and G-actin was present at the same concentration as either the displaced or displacing compound, whichever was lower. For example, when displacing CapG from G-actin with compound **5**, CapG and G-actin were at 25 nM, and **5** was at 20 μM. The emission spectra were taken from 410 to 650 nm (16 nm bandwidth, 54.7° polarization) by using an AB2 fluorimeter with excitation at 385 nm (8 nm bandwidth, 0° polarization).

Cell Assays

NBT-II cells (ATCC) were cultured as previously described by Choidas et al. (1998). Cells were treated with the compounds overnight before being imaged with a phase-contrast microscope.

ACKNOWLEDGMENTS

This work was supported by grants awarded to G.M. from the National Institutes of Health (R01 EB005217-01 and R01 HL069970-01) and I.P. from the Engineering and Physical Sciences Research Council (GR/S19929/01) and Merck Research Laboratories (Scholarship to G.C.).

Received: December 5, 2007
Revised: January 22, 2008
Accepted: January 28, 2008
Published: March 21, 2008

REFERENCES

Allingham, J.S., Tanaka, J., Marriott, G., and Rayment, I. (2004). Absolute stereochemistry of ulapualide A. Org. Lett. *6*, 597–599.

Allingham, J.S., Zampella, A., D'Auria, M.V., and Rayment, I. (2005). Structures of microfilament destabilizing toxins bound to actin provide insight into toxin design and activity. Proc. Natl. Acad. Sci. USA *102*, 14527–14532.

Bradford, M.M. (1976). A rapid and sensitive method for the quantitation of microgram quantities of protein utilizing the principle of protein-dye binding. Anal. Biochem. *72*, 248–254.

Choidas, A., Jungbluth, A., Sechi, A., Murphy, J., Ullrich, A., and Marriott, G. (1998). The suitability and application of a GFP-actin fusion protein for long-term imaging of the organization and dynamics of the cytoskeleton in mammalian cells. Eur. J. Cell Biol. *77*, 81–90.

D'Auria, M.V., Paloma, L.G., Minale, L., Zampella, A., Verbist, J.F., Roussakis, C., Debitus, C., and Patissou, J. (1994). Reidispongiolide-A and reidispongiolide-B, two new potent cytotoxic macrolides from the New-Caledonian sponge *Reidispongia Coerulea*. Tetrahedron *50*, 4829–4834.

Dominguez, R. (2004). Actin-binding proteins—a unifying hypothesis. Trends Biochem. Sci. *29*, 572–578.

Fenteany, G., and Zhu, S. (2003). Small-molecule inhibitors of actin dynamics and cell motility. Curr. Top. Med. Chem. *3*, 593–616.

Goldschmidt-Clermont, P.J., Machesky, L.M., Baldassare, J.J., and Pollard, T.D. (1990). The actin-binding protein profilin binds to Pip2 and inhibits its hydrolysis by phospholipase-C. Science *247*, 1575–1578.

Goldschmidt-Clermont, P.J., Furman, M.I., Wachsstock, D., Safer, D., Nachmias, V.T., and Pollard, T.D. (1992). The control of actin nucleotide exchange by thymosin-β-4 and profilin—a potential regulatory mechanism for actin polymerization in cells. Mol. Biol. Cell *3*, 1015–1024.

Gordon, D.J., Yang, Y.-Z., and Korn, E.D. (1976). Polymerization of *Acanthamoeba* actin. Kinetics, thermodynamics, and co-polymerization with muscle actin. J. Biol. Chem. *251*, 7474–7479.

Haddad, J.G., Harper, K.D., Guoth, M., Pietra, G.G., and Sanger, J.W. (1990). Angiopathic consequences of saturating the plasma scavenger system for actin. Proc. Natl. Acad. Sci. USA *87*, 1381–1385.

Hirata, K., Muraoka, S., Suenaga, K., Kuroda, T., Kato, K., Tanaka, H., Yamamoto, M., Takata, M., Yamada, K., and Kigoshi, H. (2006). Structure basis for antitumor effect of aplyronine A. J. Mol. Biol. *356*, 945–954.

Kigoshi, H., Suenaga, K., Takagi, M., Akao, A., Kanematsu, K., Kamei, N., Okugawa, Y., and Yamada, K. (2002). Cytotoxicity and actin-depolymerizing activity of aplyronine A, a potent antitumour macrolide of marine origin, and its analogs. Tetrahedron *58*, 1075–1102.

Klenchin, V.A., Allingham, J.S., Kin, R., Tanaka, J., Marriott, G., and Rayment, I. (2003). Trisoxazole macrolide toxins mimic the binding of actin-capping proteins to actin. Nat. Struct. Biol. *10*, 1058–1063.

Marriott, G., Zechel, K., and Jovin, T.M. (1988). Spectroscopic and functional characterization of an environmentally sensitive fluorescent actin conjugate. Biochemistry *27*, 6214–6220.

Mounzer, K.C., Moncure, M., Smith, Y.R., and Dinubile, M.J. (1999). Relationship of admission plasma gelsolin levels to clinical outcomes in patients after major trauma. Am. J. Respir. Crit. Care Med. *160*, 1673–1681.

Otterbein, L.R., Graceffa, P., and Dominguez, R. (2001). The crystal structure of uncomplexed actin in the ADP state. Science *293*, 708–711.

Paterson, I., Ashton, K., Britton, R., Cecere, G., Chouraqui, G., Florence, G.J., and Stafford, J. (2007). Total synthesis of (-)-reidispongiolide A, an actin-targeting marine macrolide. Angew. Chem. Int. Ed. Engl. *46*, 6167–6171.

Paterson, I., Ashton, K., Britton, R., Cecere, G., Chouraqui, G., Florence, G.J., Knust, H., and Stafford, J. (2008). Total synthesis of (-)-reidispongiolide A, an actin-targeting macrolide isolated from the marine sponge *Reidispongia coerulea*. Chem. Asian J. *3*, 367–387.

Petchprayoon, C., Suwanborirux, K., Tanaka, J., Yan, Y.L., Sakata, T., and Marriott, G. (2005). Fluorescent kabiramides: New probes to quantify actin in vitro and in vivo. Bioconjug. Chem. *16*, 1382–1389.

Petchprayoon, C., Asato, Y., Higa, T., Garcia-Fernandez, L.F., Pedpradab, S., Marriott, G., Suwanborirux, K., and Tanaka, J. (2006). Four new kabiramides from the Thai sponge, *Pachastrissa nux*. ChemInform *69*, 447–456.

Roesener, J.A., and Scheuer, P.J. (1986). Ulapualide A and B, extraordinary antitumor macrolides from nudibranch eggmasses. J. Am. Chem. Soc. *108*, 846–847.

Roy, P., Raijfur, Z., Jones, D., Marriott, G., Loew, L., and Jacobson, K. (2001). Local photorelease of caged thymosin β4 in locomoting keratocytes causes cell turning. J. Cell Biol. *153*, 1035–1048.

Smith, D.B., Janmey, P.A., Sherwood, J.A., Howard, R.J., and Lind, S.E. (1988). Decreased plasma gelsolin levels in patients with *Plasmodium falciparum* malaria: a consequence of hemolysis? Blood *72*, 214–218.

Southwick, F.S., and DiNubile, M.J. (1986). Rabbit alveolar macrophages contain a Ca^{2+}-sensitive, 41,000-dalton protein which reversibly blocks the "barbed" ends of actin filaments but does not sever them. J. Biol. Chem. *261*, 14191–14195.

Tanaka, J., Yan, Y., Choi, J., Bai, J., Klenchin, V.A., Rayment, I., and Marriott, G. (2003). Biomolecular mimicry in the actin cytoskeleton: mechanisms underlying the cytotoxicity of kabiramide C and related macrolides. Proc. Natl. Acad. Sci. USA *100*, 13851–13856.

Weber, G., and Farris, F. (1979). Synthesis and spectral properties of a hydrophobic fluorescent probe: 6-propionyl-2-(dimethylamino)naphthalene. Biochemistry *18*, 3075–3078.

Westphal, M., Jungbluth, A., Heidecker, M., Muhlbauer, B., Heizer, C., Schwartz, J.M., Marriott, G., and Gerisch, G. (1997). Microfilament dynamics during cell movement and chemotaxis monitored using a GFP-actin fusion protein. Curr. Biol. *7*, 176–183.

Yeung, K.-S., and Paterson, I. (2002). Actin-binding marine macrolides: total synthesis and biological importance. Angew. Chem. Int. Ed. Engl. *41*, 4632–4653.

Zechel, K. (1993). The interaction of 6-propionyl-2-(NN-dimethyl)aminonaphthalene (PRODAN)-labeled actin with actin-binding proteins and drugs. Biochem. J. *290*, 411–417.

Zhang, Y., Vorobiev, S.M., Gibson, B.G., Hao, B.H., Sidhu, G.S., Mishra, V.S., Yarmola, E.G., Bubb, M.R., Almo, S.C., and Southwick, F.S. (2006). A CapG gain-of-function mutant reveals critical structural and functional determinants for actin filament severing. EMBO J. *25*, 4458–4467.

